ELSEVIER

Ceramics International 33 (2007) 13–20

CERAMICS INTERNATIONAL

www.elsevier.com/locate/ceramint

Impedance spectroscopy studies on Fe^{3+} ion modified PLZT ceramics

Soma Dutta [a], R.N.P. Choudhary [a], P.K. Sinha [b,*]

[a] *Department of Physics and Meteorology, Indian Institute of Technology, Kharagpur 721302, India*
[b] *Department of Aerospace Engineering, Indian Institute of Technology, Kharagpur 721302, India*

Received 20 December 2004; received in revised form 5 May 2005; accepted 14 July 2005
Available online 10 October 2005

Abstract

Polycrystalline Fe^{3+}-modified PLZT $Pb_{0.92}(La_{0.1}Fe_{0.9})_{0.08}(Zr_{0.60}Ti_{0.40})_{0.98}O_3$ (PLFZT) was prepared by high temperature solid-state reaction. Preliminary room temperature X-ray study confirms the formation of single-phase compounds in a tetragonal crystal system. The electrical behavior (complex impedance Z^*, complex permittivity ε^*, complex modulus M^*) of the PLFZT system has been studied by non-destructive complex impedance spectroscopy (CIS). Grain and grain boundary conduction is observed from complex impedance spectrum at high temperatures (650 K and above) by the appearance of two semicircular arcs. The Cole–Cole plots of permittivity spectrum consisted of a circular arc followed by a semicircular spur indicate that the dielectric phenomenon of PLFZT is due to conductive grain boundaries. This is quite different in nature from Debye type mono dispersive phenomenon. The temperature variation of real permittivity gives evidence of the ferroelectric phase transition as well as of the relaxation behavior. The presence of non-Debye type multiple relaxations has been confirmed by complex modulus analysis.

Keywords: C. Electrical conductivity; C. Ferroelectric properties; D. PLZT; Impedance spectroscopy

1. Introduction

Ferroelectric materials with perovskite structures have received much attention due to their excellent functional properties, such as piezoelectricity, pyroelectricity, electro-optic effects, useful for devices. Since the discovery of lanthanum-modified lead zirconate-titanate (PLZT) ceramics with high optical transparency and good electro optical and other characteristics, numerous interests have been generated on the materials for possible applications in optical devices [1–5]. Depending on the chemical composition of PLZT, various ferroelectric/antiferroelectric or paraelectric phases with slightly different dielectric properties and crystal structures of different type are formed. In all ferroelectrics, in general, the study of electrical conductivity is very important to realize the associated physical properties and nature of conductivity in these materials. On the other hand, study of electrical properties of PLZT using complex impedance spectroscopy (CIS) technique has received little attention [6,7].

The CIS is a powerful technique to characterize many electrical properties of materials. It is useful to evaluate and separate the contribution of the overall electrical properties in the frequency domain due to electrode reactions at the electrode/sample interface and migration of ions through the grains and across the grain boundaries in a polycrystalline material.

Detailed literature survey reveals that not much work has been done on Fe-modified PLZT ceramics [8]. However, impedance studies, i.e., electrical properties and frequency response at different temperatures of Fe-modified PZT and related materials have hardly been reported in the literature [9,10]. Recently, the structural and dielectric properties of PLZT with the varying concentration of Fe^{3+} ion have thoroughly been studied by us [11]. In view of the interesting results, we report here our studies on electrical properties (material impedance, electrical relaxation process, dielectric behavior, electrical modulus, etc.) of the PLFZT system using complex impedance spectroscopy technique.

* Corresponding author. Tel.: +91 3222 283016; fax: +91 3222 255303.
E-mail address: pksinha@aero.iitkgp.ernet.in (P.K. Sinha).

0272-8842/$30.00
doi:10.1016/j.ceramint.2005.07.010

2. Background

The CIS is a non-destructive experimental technique for the characterization of micro structural and electrical properties of some electronic materials [12]. The technique is based on analyzing the ac response of a system to a sinusoidal perturbation and subsequent calculation of impedance as a function of the frequency of the perturbation. The analysis of the electrical properties (conductivity, dielectric constant/loss, etc.) carried out using relaxation frequency (ω_{max}) values gives unambiguous results when compared with those obtained at arbitrarily selected fixed frequencies. The frequency dependent properties of a material can be described as complex permittivity (ε^*), complex impedance (Z^*), complex admittance (Y^*), complex electric modulus (M^*) and dielectric loss or dissipation factor (tan δ). The real (ε', Z', Y', M') and imaginary (ε'', Z'', Y'', M'') parts of the complex parameters are in turn related to one another as follows:

$\varepsilon^* = \varepsilon' - j\varepsilon''$ as :

$$\varepsilon' = -\frac{Z''}{\omega C_0(Z'2 + Z''2)} \quad (1)$$

$$\varepsilon'' = \frac{Z'}{\omega C_0(Z'2 + Z''2)} \quad (2)$$

$$M^* = M' + jM'' = \frac{1}{\varepsilon^*} = j\omega\varepsilon_0 Z^* \quad (3)$$

$$Z^* = Z' - jZ'' = \frac{1}{jC_0\varepsilon^*\omega} \quad (4)$$

$$Y^* = Y' + jY'' = j\omega C_0\varepsilon^* \quad (5)$$

$$\tan\delta = \frac{\varepsilon''}{\varepsilon'} = \frac{M''}{M'} = \frac{Z'}{Z''} = \frac{Y'}{Y''} \quad (6)$$

where $\omega = 2\pi f$ is the angular frequency, C_0 is the geometrical capacitance, $j = \sqrt{-1}$. These relations offer wide scope for a graphical analysis of the various parameters under different conditions of temperature or frequency. The useful separation of intergranular phenomena depends ultimately on the choice of an appropriate equivalent circuit to represent the sample properties.

3. Experiment

Polycrystalline sample of $Pb_{0.92}(La_{0.1}Fe_{0.9})_{0.08}(Zr_{0.60}Ti_{0.40})_{0.98}O_3$ was prepared by a high-temperature solid-state reaction technique using high purity ingredient oxides in the required stoichiometry. These ingredients were thoroughly mixed in wet (methanol) medium for 6 h. The mixture was calcined in a high purity alumina crucible at 1325 K for 7 h in an air atmosphere and brought to room temperature under slow cooling. The process of calcination and mixing was repeated until the formation of the compound was confirmed by XRD technique. The calcined powder was pelletized into a disk using polyvinyl alcohol (PVA) as binder. Finally the disks were sintered at 1525 K for 24 h in a platinum crucible in $PbZrO_3$ atmosphere to prevent the lead loss at high temperature.

The X-ray powder diffraction pattern of the sample was recorded on calcined powder over a wide range of Bragg angles ($20^\circ \leq 2\theta \leq 80^\circ$) at room temperature using a Philips (PW 1710) X-ray powder diffractometer (with Co Kα radiation, $\lambda = 1.7902$ Å) with a scanning rate of 2° min^{-1}.

For electrical characterizations, the sintered disks were polished to make both the faces flat and parallel and electroded with high-purity air-drying conducting silver paste. The impedance measurements were taken. Measurements were made isothermally allowing thermal equilibrium by leaving the furnace at the preset temperature for 30 min on these disk samples and the data were recorded using computer-controlled Hioki 3532 LCR Hitester, over a wide range of temperature (305–750 K) and frequency (0.1–10^3 kHz) with an applied voltage of 1.3 V. Measurements provided the real and imaginary parts of the impedance and dielectric as frequency-dependent values.

4. Results and discussion

4.1. Structural

Fig. 1 shows the comparative changes in the basic XRD pattern of the PLZT material with the 9% replacement of the La ion by the Fe ion. On Fe doping in PLZT the following changes were observed in the X-ray diffraction pattern; (i) shift in peak position (ii) increase in peak (1 0 1) intensity (iii) appearance of a shoulder, i.e., peak splitting towards the lower angle side (iv) peak broadening. All the observed peaks were indexed and lattice parameters were determined using a least-squares standard computer program "POWD" [13]. On the basis of the best agreement between observed and calculated interplanar spacing (d_{obs} and d_{cal}), a suitable unit cell of the Fe doped PLZT compound was selected in tetragonal crystal system with $a = 4.053$ Å and $c = 4.087$ Å whereas the cell parameters for PLZT was found $a = 4.009$ and $c = 4.013$. The tetragonality (c/a) is increased by 1% on

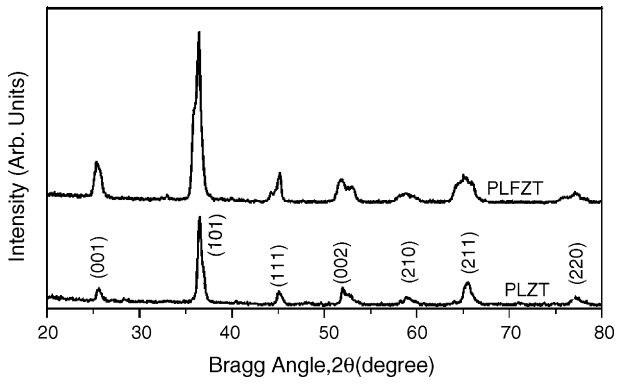

Fig. 1. XRD patterns of PLZT, PLFZT material.

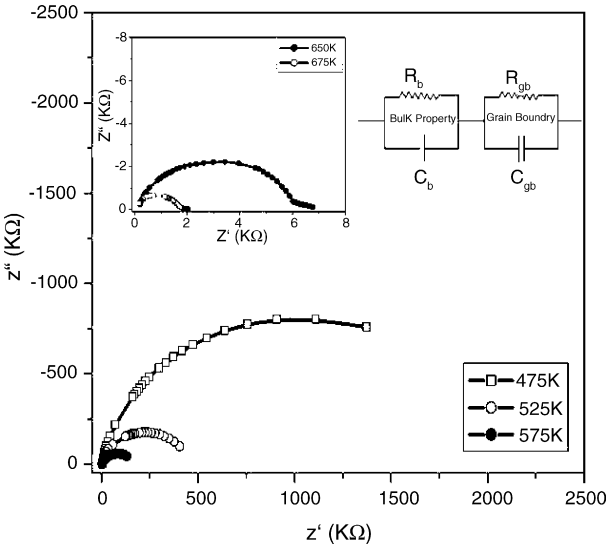

Fig. 2. Nyquist plot of PLFZT material.

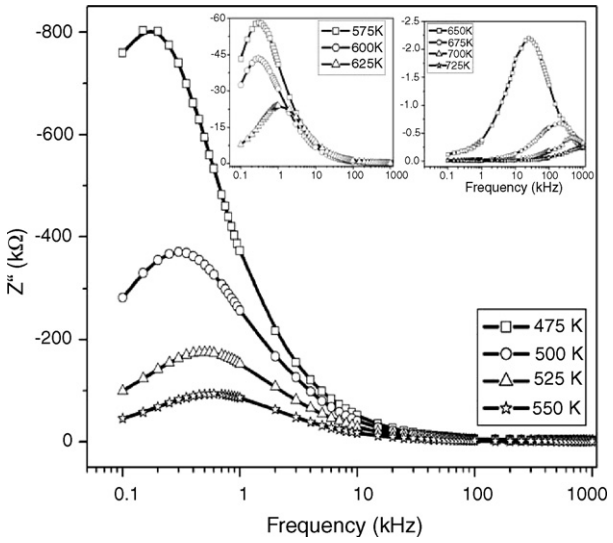

Fig. 3. Plot of imaginary part of impedance with frequency of PLFZT.

Fe doping at PLZT. A tetragonal splitting at higher Bragg angle is observed in the diffraction peaks which justify the selection of the tetragonal crystal system. So from XRD analysis of the material it can be concluded that basic crystal structure of PLZT (60/40) is remained unaltered on the Fe substitution at the La-site. A slight distortion in the unit cell (1%) and increase in volume (5%) is observed due to 9% replacement of the La ion by Fe.

4.2. Complex impedance study

Fig. 2 shows the complex impedance spectrum of PLFZT at five different temperatures. The change in temperature ensures a distinct effect on the characteristics impedance spectrum of the material by the appearance of low temperature single semicircular arc arised due to the bulk properties of the material and high temperature (600 K and above) double semicircular arcs (inset Fig. 2) due to the consequence of the bulk and grain boundary conduction. These semicircular arcs appear in distinct frequency ranges, one at a higher frequency followed by another lower frequency semicircular arc. This feature is almost similar at different temperatures, also with a difference in radii of curvature of the arcs, which reduces with rise in temperature. The semicircular pattern in the impedance spectrum is a representative of the electrical processes taking place in the material which can be expressed as an equivalent electrical circuit comprising of a parallel combination of resistive and capacitive elements. The presence of two semicircular arcs accordingly can be thought of as resulting from cascading effect of parallel combination of resistive and capacitive elements arising due to the contribution of bulk property of the material and grain boundary effect. The high frequency semicircle is attributed to the bulk property of the material (parallel combination of bulk resistance and bulk capacitance), and low frequency semicircle is due to the grain boundary effects in the material (parallel combination of grain boundary resistance and capacitance). The electrical processes taking place within the material has been modeled on for a polycrystalline system and is shown in terms of the equivalent electrical circuit in the Fig. 2 (inset).

Fig. 3 shows the variation of Z'' with frequency at different temperatures. A broad peak appears irrespective to the temperatures. The average peak position regularly shifts towards higher frequency as the temperature increases. This insures the temperature dependent relaxation process in the sample. Furthermore, as evident from the plots, as the temperature increases the magnitude of Z'' decreases, the effect being to be more pronounced at the peak position. The shift of the peak towards higher frequency in raising the temperature is possibly due to the reduction in the bulk resistivity. The asymmetric peaks suggest the presence of electrical processes in the material with spread of relaxation time. The relaxation species may possibly be electrons or immobile species at lower temperature and defects at higher temperature that may be responsible for electrical conduction in the material.

Effectively large values of Z' and Z'' at low frequencies or temperatures indicates a predominant effect of the polarizations which is consistent of large ε values of PLZTs. The intercepts of the two semicircles are used to calculate the bulk resistance (R_b) and grain boundary resistance (R_{gb}) while the corresponding frequency value evaluated from the apex of the semicircles have been used to calculate the bulk and grain boundary capacitance (C_b) using the relation,

$$\omega_{max} C_b R_b = 1 \text{ or, } \omega_{max} C_{gb} R_{gb} = 1 \quad (7)$$

for a parallel combination of R and C. As temperature increases, both the grain resistance (R_b) and grain boundary resistance (R_{gb}) is found to decrease with rise in temperature indicated by a shift in the radius of the semicircular arcs

Table 1
Comparison of bulk capacitance (C_b), relaxation time (τ) and full width at half maximum (FWHM) calculated from complex modulus data at different temperatures

T (K)	C_b (nF)	τ (s)	FWHM (decade)
475	0.42	1.06×10^{-3}	–
525	0.67	3.2×10^{-4}	–
575	1.36	2.31×10^{-4}	–
650	1.01	6.36×10^{-6}	1.61
675	0.41	7.95×10^{-7}	1.35
700	0.1	3.53×10^{-7}	1.24

towards left side on the real (Z') axis with increase in temperature. This provides convincing evidence that the electrical properties of PLZT are dependant on microstructure as well as temperature.

A single nondegenarate process involves a single nondegenarate relaxation time

$$\tau = C_b R_b = \frac{1}{\omega} \tag{8}$$

for a given set of R_b and C_b at a temperature. The value of τ determined at selected temperatures in the region of measuring temperature using the values of R_b and C_b in Eq. (8) is listed in Table 1. The τ-value is found to be decreasing linearly on increasing value of the temperature (above 575 K) suggesting a typical semiconductor behavior. The variation of τ with temperature (Fig. 4) implies that the relaxation process is temperature dependent. The activation energy E_a evaluated from the slope of the curve by the relation,

$$\tau = \tau_0 e^{-E_a/kT} \tag{9}$$

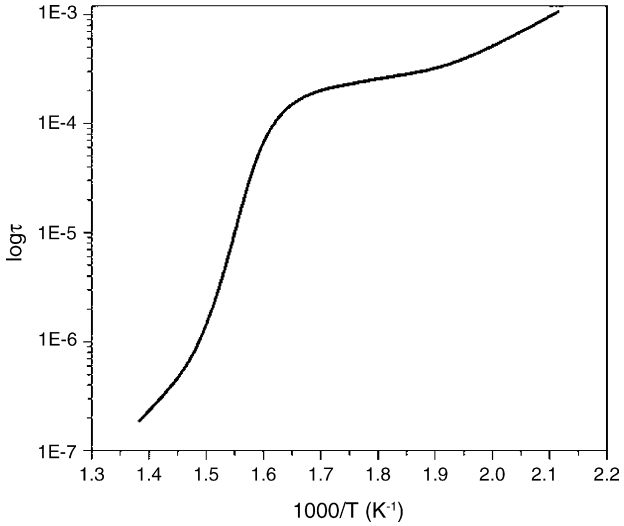

Fig. 4. Plot of relaxation time with 1000/T of PLFZT.

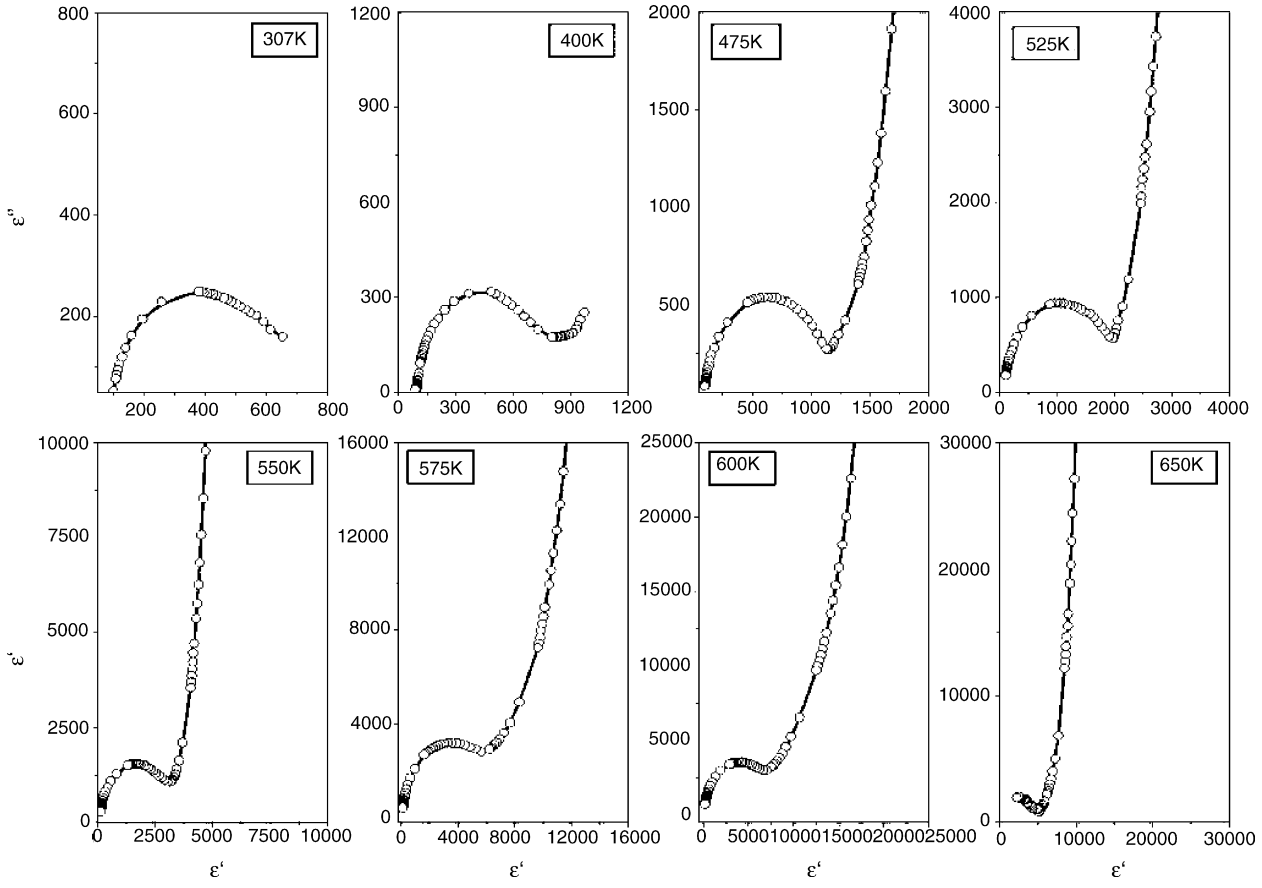

Fig. 5. Complex permittivity (Cole–Cole) plot PLFZT.

where τ_0 pre exponential factor, E_a activation energy, k the Boltzmann constant and T the absolute temperature, is found to be 0.47 eV below 575 K and 2.6 eV above 575 K.

4.3. Complex permittivity study

The technique of impedance analysis has enabled us to separate the real and imaginary parts of dielectric constant in accordance with the relations (1) and (2). The values so obtained are expressed in the form of complex permittivity, was developed by Cole and Cole [14] (Fig. 5). The figure indicate a polydispersive nature of dielectric phenomenon in PLFZT with the possibility of distributed relaxation time as indicated by the presence of semicircular arcs at different temperatures with their center located below the real (ε') axis. The complex dielectric spectrum of this nature is well described by the empirical relation developed by Cole–Cole and expressed as:

$$\varepsilon^* = \varepsilon' - j\varepsilon'' = \varepsilon_\infty + \frac{\varepsilon_s - \varepsilon_\infty}{1 + (i\omega\tau)^{1-h}} = \varepsilon_\infty + \frac{\Delta\varepsilon}{1 + (i\omega\tau)^{1-h}} \tag{10}$$

where $\Delta\varepsilon = \varepsilon_s - \varepsilon_\alpha$ is the dielectric relaxation strength, τ is the characteristics relaxation time and h is the parameter describing the distribution of relaxation time. Here, $h = 0$ describes mono dispersive relaxation, while $0 < h < 1$ indicates a distribution of relaxation times in the system. Clearly the Cole–Cole plot indicates that dielectric phenomenon is different from Debye type mono dispersive phenomenon.

Further, the complex permittivity plots have been observed to become progressively more circular with rise in temperature. They are also characterized by the appearance of another semicircular spur in the low frequency region, which may be attributed possibly to the diffusion phenomenon of Warburg type arising due to ion migration at higher temperatures. This result possibly indicates that with rise in temperature the intrinsic property of the material changes with loss in polarization process resulting in the mobility of cations. This appears reasonable because the presence of La^{3+} at the Pb^{2+} site leads to increase in the Pb^{2+} vacancies in the perovskite structure resulting in possible creation of vacancies favouring a preferred La^{3+} diffusion into Ti^{4+} rich composition [15]. This type of behavior is typical to dielectric ceramics having conductive grain boundary arising out of a relaxation process of the Maxwell–Wagner type.

The real (ε') and imaginary (ε'') components of the relative permittivity of PLFZT in a wide temperature range is shown in Fig. 6(a) and (b) where the real and imaginary components are plotted on a linear scale against the logarithm of frequency. The magnitude of ε' decreases increasing frequency (Fig. 6(a)) which is a typical characteristic of any ferroelectric material.

The prevailing form of frequency dependence of the dielectric loss peaks may be represented by the empirical

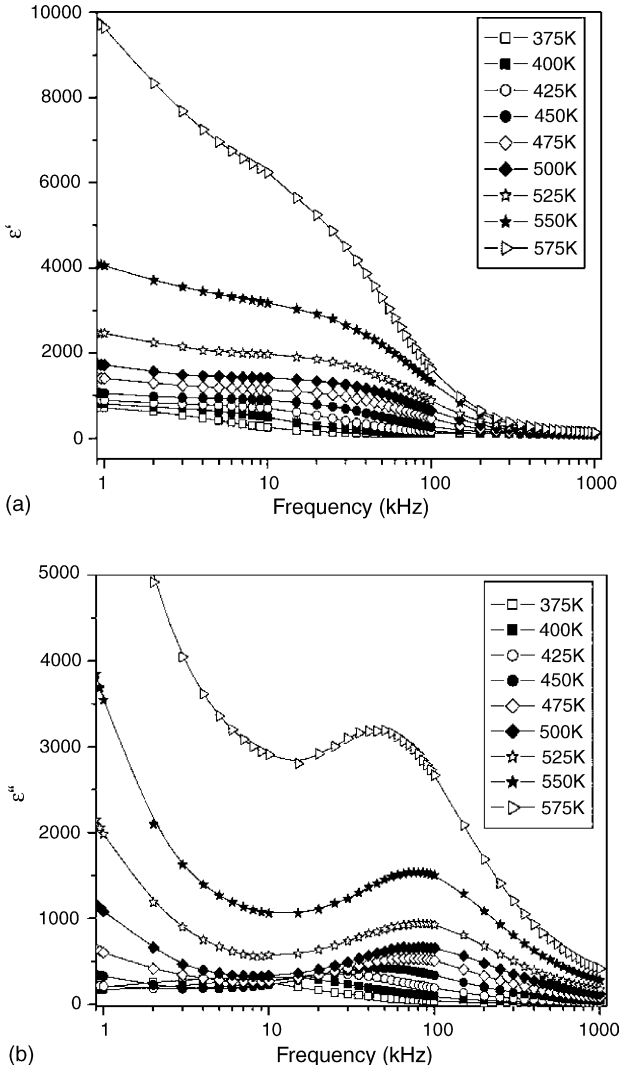

Fig. 6. (a) Plot of real part of permittivity (ε') with frequency of PLFZT material. (b) Plot of imaginary part of permittivity (ε'') with frequency of PLFZT material.

law combining two power laws (ω^{n-1}, $n < 1$), respectively, below and above the peak frequency (ω_p)

$$\varepsilon''(\omega) \propto \frac{1}{(\omega/\omega_p)^{-m} + (\omega/\omega_p)^{1-n}} \tag{11}$$

in which exponents m and n lie in the range of 0–1 and the peak frequency is generally temperature dependent. This empirical relation is applicable only at lower frequencies while at high frequencies perturbing processes arising due to presence of some series resistance in the measuring system or overlap of some other loss processes. So, dielectric loss of the material may be explained in better way using a law corresponding to the second term in Eq. (11) over a wide range of frequencies assuming the conduction caused by hoping charge carriers to some extent [16]. So over a wide range of frequencies the dielectric loss follows a universal law of loss

$$\varepsilon''(\omega) = B(T)\omega^{n(T)-1} \tag{12}$$

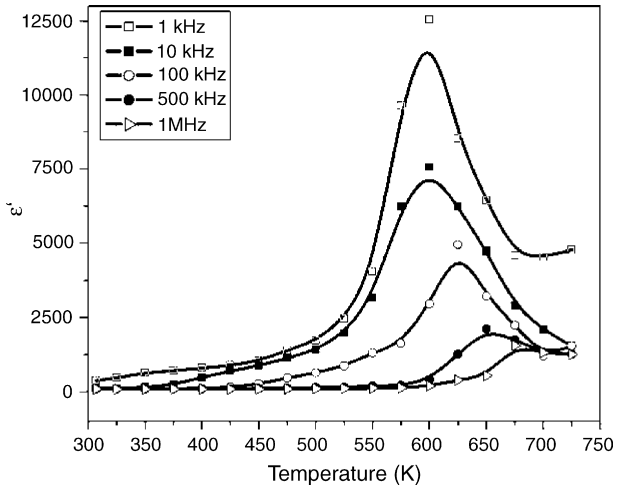

Fig. 7. Variation of dielectric permittivity (ε') with temperature of PLFZT material.

where $B(T)$ is a temperature dependent parameter.

According to Kramers–Kronig relations, the empirical relation for $\varepsilon''(\omega)$ implies the same frequency depence as for $\varepsilon'(\omega)$ in which the ratio of $\varepsilon''(\omega)/\varepsilon'(\omega)$ is a constant (i.e., independent of frequency). In the present study, the calculated dielectric constant from the experimental data plots is far off from the Debye relaxation type for which it is equal to $\omega\tau$ [12].

The variation of real permittivity with temperature is shown in Fig. 7. It appears that the temperature dependence of real dielectric constant (ε') at different frequencies have typical features of relaxor ferroelectrics: (i) the value of ε' increases gradually with rise in temperature and reached to a maximum value $\varepsilon'_{\max}$ at a particular temperature known as Curie temperature (T_c). This general feature is similar at all frequencies, (ii) the value of $\varepsilon'_{\max}$ at T_c decreases with increasing frequency. Further its value is larger at lower frequency (1 kHz), (iii) the value of T_c shifts towards the higher temperature side with increase in frequency and (iv) the dielectric dispersion is absent at high temperatures beyond T_c where as the dielectric constant has been observed to decrease with increasing frequencies at temperatures around and lower than T_c. This indicates strong dielectric dispersion at temperatures around and below T_c. The T_c value shifts from 600 to 650 K with the increased frequency value 1 kHz to 1 MHz. These features suggest that the ε' in PLFZT originates possibly as a result of the combined effect of relaxation polarization and resonance polarization processes [17] and is governed by the relations:

$$\varepsilon_m(\omega,T) = \varepsilon_1(\omega,T) + \varepsilon_2(\omega,T);$$
$$\text{with } \varepsilon_1(\omega,T) = \frac{\varepsilon_H(T)}{1 + D_1[\varepsilon_H(T)/A(T)\ln\omega_0]^m}; \quad (13)$$
$$\varepsilon_2(\omega,T) = \frac{\varepsilon_1(\omega,T)}{1 + D_2[A(T)\ln\omega_0/\varepsilon_H(T)]^n}$$

ε_m = total measured dielectric response of the material, ε_1 = dielectric response related to relaxation polarization, ε_2 = dielectric response related to resonance polarization, ε_H and ε_L are the measured dielectric constant at high and low temperatures. D_1 and D_2 are frequency dependent constants m (>1), n (>1), and are independent of both temperature and frequency.

As temperature rises, the thermally activated flips of polar regions (also known as super paraelectrics) and their interaction in the material lead to a gradual increase in the permittivity of the system. The appearance of dielectric peak may be attributed to phase transition (ferroelectric–paraelectric) in the material. On further rise in temperature, there is a rapid loss of the polarization in the material. This result in the monotonous fall of dielectric constant with rise in temperature beyond T_c [18,19]. It also appears that the dielectric constant is higher at the lower frequency.

4.4. Complex modulus study

The complex modulus spectrum indicates electrical phenomenon with the smallest capacitance occurring in a dielectric system. Fig. 8 represents complex modulus spectrum of PLFZT at different temperatures. The appearance of a single arc in the spectrum at different temperatures confirms the single-phase character of PLFZT. This observation agrees well with the results of preliminary XRD analysis. The modulus data expressed in the complex modulus formalism:

$$M^* = \frac{1}{\varepsilon^*} = j(\omega C_0)Z^*; \quad j = (-1)^{1/2} \quad (14)$$

enables us to understand the phenomenon of conductivity relaxation in terms of the variation of M'' as a function of frequency.

The modulus master curve is shown in Fig. 9 that enables us to have an insight into the dielectric processes occurring in the material as a function of temperature. The master modulus curve indicates a considerable shift in modulus

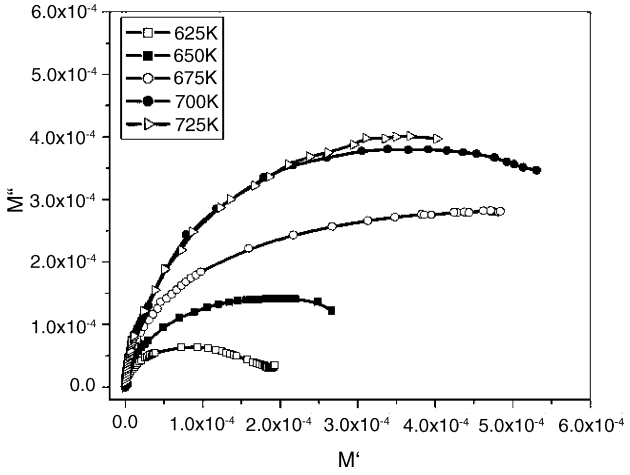

Fig. 8. Complex modulus plot of PLFZT material.

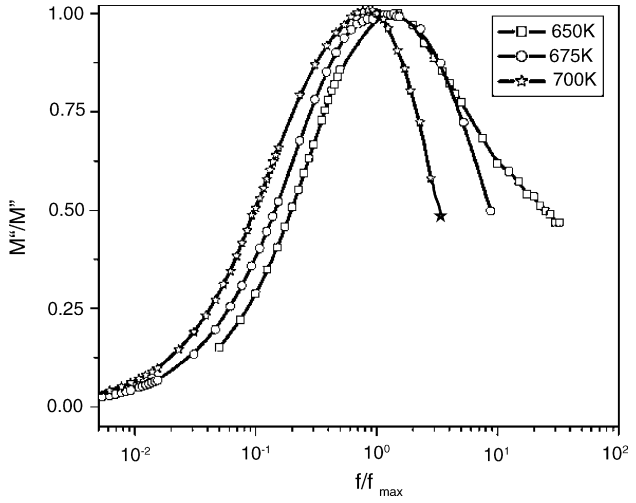

Fig. 9. Modulus master curve for PLFZT material.

peak pattern and basically the similar shape and pattern with slight variation in full width at half maximum (FWHM) with rise in temperature. The value of FWHM as evaluated from the normalized modulus spectrum when compared with that of a Debye peak (1.14 decade) gives a fairly accurate estimate of β. The value of β estimated in the present studies using the value of FWHM (Table 1) suggests non-Debye type relaxation phenomena in good agreement with the observations from complex permittivity spectrum of multiple relaxations. Also the lowering in the value of β at high temperature (700 K) may indicate that the most of the charge species have been relaxed at the elevated temperature and the system is approaching towards the monodispersive (Debye) type.

The variation of normalized parameters M''/M''_{max} and Z''/Z''_{max} as a function of logarithmic frequency measured at 650 K is presented in Fig. 10. The peak frequency shifts towards higher frequency region as it moves from M'' to Z''.

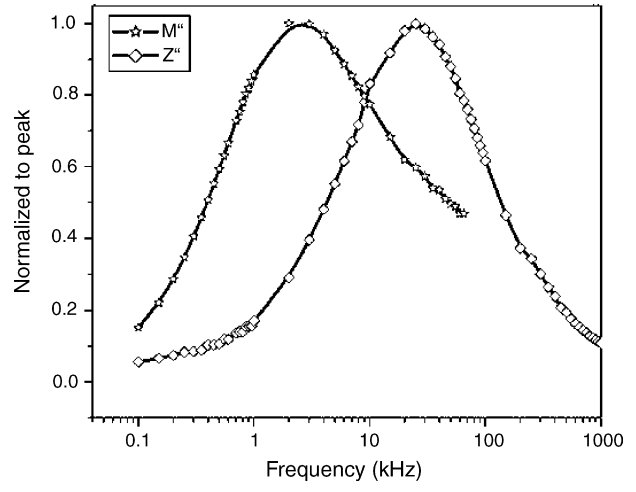

Fig. 10. Logarithmic plot of normalized parameters (M'', Z'') at 650 K.

The magnitude of mismatch between the peaks of both parameters represents a change of the apparent polarization [20]. The difference in peak position of normalized parameters is an evident of short-range conductivity [19]. The very distinct curves of M''/M''_{max} and Z''/Z''_{max} (Fig. 10) illustrates clearly that polarization process is due to a localized conduction of multiple carriers that describes the presence of multiple relaxation process in the material. Normally dielectric material contains a certain density of localized charges, some of which may be able to hop over many consecutive sites ultimately giving rise to a dc conductivity, while others may be restricted to shorter ranges, with the limiting case of pairs of hopping sites. Again the lower value of $\varepsilon_s/\varepsilon_\infty$ (in the region of 425–625 K) at all the temperatures region follows the short-range conduction of the material due to hopping at low temperatures and defects at higher temperature region.

5. Conclusions

Polycrystalline PLFZT has been studied by a complex impedance spectroscopy technique. Structural and electrical properties of the material have been estimated from impedance data. These results have been expressed in terms of complex impedance spectrum, complex permittivity spectrum, complex modulus spectrum and conductivity spectrum. Modulus analysis has confirmed the single-phase behavior of the materials in a good agreement with the information received from XRD study. The dielectric processes in the materials have been shown to be due to the existence of relaxation and resonance polarization and thermally activated flips of polar regions. The polydispersive nature of the dielectric phenomenon suggests the presence of distributed relaxation time in the material.

References

[1] G.H. Haertling, C.E. Land, J. Am. Ceram. Soc. 54 (1) (1971) 1.
[2] G.H. Haertling, Ferroelectrics 75 (1987) 25.
[3] Z. Xu, X.H. Dai, D. Viehland, Phys. Rev. B 51 (1995) 6261.
[4] X. Yao, Z.L. Chen, L.E. Cross, J. Appl. Phys. 54 (1983) 3399.
[5] L.E. Cross, Ferroelectrics 76 (1987) 241.
[6] A. Peláiz Barranco, F. Calderón Piñar, O. Pérez Martínez, J. De Los Santos Guerra, I. González Carmenate, J. Eur. Ceram. Soc. 19 (1999) 2677.
[7] S. Dutta, R.N.P. Choudhary, P.K. Sinha, A.K. Thakur, J. Appl. Phys. 96 (3) (2004) 1607.
[8] V.I. Dimza, J. Phys. Condens. Matter 8 (1996) 2887.
[9] B. Majumder, B. Roy, S.B. Krupanidhi, R.S. Katiyar, Appl. Phys. Lett. 79 (2001) 239.
[10] E. Boucher, D. Guyomar, L. Lebrun, B. Guiffard, G. Grange, J. Appl. Phys. 92 (9) (2002) 5437.
[11] S. Dutta, R.N.P. Choudhary, P.K. Sinha, J. Mater. Sci. Mater. Electr. 14 (8) (2003) 463.
[12] J.R. Macdonald (Ed.), Impedance Spectroscopy, Wiley, New York, 1987.

[13] E. Wu, POWD, An Interactive Powder Diffraction Interpretation and Indexing Program, Ver2.1, School of Physical Sciences, Finder's University of South Australia, Bedford Park.
[14] K.S. Cole, R.H. Cole, J. Chem. Phys. 9 (1941) 341.
[15] M. Laurent, U. Schreiner, P.A. Langjahr, A.E. Glazounov, M.J. Hoffman, J. Eur. Ceram. Soc. 21 (2001) 1495.
[16] A.K. Jonscher, Nature 250 (1974) 191.
[17] A.K. Jonscher, Nature 253 (1975) 27.
[18] Z.Y. Cheng, R.S. Katiyar, X. Yao, A.S. Bhalla, Phys. Rev. B 57 (14) (1998) 8166.
[19] X. Yao, Chen Zhili, L.E. Cross, J. Appl. Phys. 54 (6) (1983) 3399.
[20] R. Gerhardt, J. Phys. Chem. Solids 55 (12) (1994) 1491.